American Mineralogist, Volume 71, pages 1393–1398, 1986

Optical properties of a high albite (analbite)–high sanidine solid-solution series

SHU-CHUN SU,[1] PAUL H. RIBBE, F. DONALD BLOSS, JULIE K. WARNER[2]
Department of Geological Sciences, Virginia Polytechnic Institute and State University, Blacksburg, Virginia 24061, U.S.A.

ABSTRACT

In the solid-solution series high albite (analbite)–high sanidine, it was impossible to select a set of specimens that were free from minor constituents (anorthite, celsian, Sr- and Rb-feldspars, and Fe), totally free of evidences of exsolution, and all of precisely the same structural state. So data were gathered for 32 feldspars whose range of structural states was $0.5 \leq \Sigma t_1 \leq 0.65$ (average 0.60), where $\Sigma t_1 \equiv 2t_1$ for monoclinic and $\Sigma t_1 \equiv (t_1o + t_1m)$ for triclinic feldspars, and t is the Al content of the T_1, T_1O, and T_1m sites. Only specimens determined to be at least 95% homogeneous were used, and corrections to the refractive indices were made for nonbinary constituents. The resulting refractive index curves—not labeled conventionally as n_α, n_β, and n_γ, according to magnitude, but as n_a, n_b, and n_c, according to which crystallographic axis the vibration direction is most nearly parallel—were found to change slope at $Or_{\sim 60}$. Each was adequately represented by two linear segments with different slopes, meeting at Or_{60}. The segments and inflection point correspond very closely to those representing the plot of density versus mole percent Or. As in the case of low microcline–high sanidine, the $2V_X$ versus mole percent Or curves are sigmoidal because the n_b and n_c curves cross; $2V_X = 0°$ at $Or_{\sim 73}$ for $\Sigma t_1 = 0.60$. The composition for this crossover point decreases as Σt_1 decreases.

INTRODUCTION

Many attempts have been made to characterize the variation of the refractive indices (and $2V$) of alkali feldspars of "high" structural state (see a review of early literature by Hewlett, 1959, p. 534). The classic work of Spencer (1937) produced excellent sets of optical data for naturally occurring perthitic specimens and for their heat-treated and presumably homogenized equivalents. Adding six sets of data, only one of which was collected on a homogeneous specimen, Tuttle (1952, Fig. 2, p. 559; cf. Deer et al., 1963, Fig. 30, p. 60) drew straight lines through n_α, n_β, and n_γ, delineating a "sanidine-anorthoclase" series and an "orthoclase–low albite" series. Smith's Figure 8-9 (1974, p. 386) is a modified version of Tuttle's drawing with a few additional data points, but it gives limiting curves only for the low series.

To date, the careful study by Hewlett (1959) of a suite of chemically analyzed sanidines and anorthoclases is the best documented, because he not only measured refractive indices and corrected the n_α values for effects of minor components, but he also checked crystals for homogeneity by single-crystal X-ray methods and reported d-spacings determined from powder-diffraction patterns. He used d_{201} as an independent measure of Ab content (note that strain may affect this parameter) and was the first to use d_{001} and d_{010} as measures of the degree of (Al,Si) order. Hewlett combined some of Spencer's data with his own to prepare a semiquantitative picture of the relationships among optical properties, composition, and (Al,Si) ordering in alkali feldspars. A notable contribution was his recognition that structural state is directly related to partial birefringence "b" $-$ n_α, where "b" is the principal refractive index whose vibration direction is most nearly parallel to the **b** crystallographic axis.

However, as far as the high albite–high sanidine series is concerned, the relationships between refractive indices and composition have remained confusing, at best, and the various attempts to summarize and/or simplify them for determinative purposes (e.g., Bambauer et al., 1979, Fig. 223–232, p. 123; Shelley, 1985, Fig. 9.61, p. 182; Phillips and Griffen, 1981, Fig. 7-20, p. 342) are misleading.

FACTORS AFFECTING REFRACTIVE INDICES

In addition to minor chemical constituents, a number of factors have combined to obscure the correct relationship between refractive indices and Or content in the high albite (analbite)–high sanidine series. These include the mixing of specimens with widely different structural states in the data set upon which analyses and conclusions were based, the way in which the structural state was quantified, and the convention used to label the principal refractive indices. First, let us define what is meant by "high" structural state.

[1] Permanent address: Institute of Geology, Chinese Academy of Sciences, Beijing, People's Republic of China.

[2] Present address: Department of Geology, University of New Mexico, Albuquerque, New Mexico 87131, U.S.A.

0003–004X/86/1112–1393$02.00

Table 1. Data of homogeneous alkali feldspars with $0.50 \leq \Sigma t_1 \leq 0.65$

No.	Sample	Or	Ab	An	Cn	Srf	Rbf	Fef	n_a	n_c	n_b	$2V_x$	Σt_1	Ref
1	MAB177	0.3 (0.3)	99.7 (99.7)	0.0	0.0	0.0	0.0	0.0	1.5276 (1.5276)	1.5346 (1.5346)	1.5364 (1.5364)	53.6	0.59	7
2	MAB169	0.3 (0.3)	99.7 (99.7)	0.0	0.0	0.0	0.0	0.0	1.5279 (1.5279)	1.5344 (1.5344)	1.5372 (1.5372)	66.1	0.64	7
3	RAMONA(H)	1.1 (1.1)	98.7 (98.9)	0.2	0.0	0.0	0.0	0.0	1.5273 (1.5272)	1.5344 (1.5343)	1.5357 (1.5356)	46.9	0.51*	4
4	DQ-1	25.2 (27.1)	67.9 (72.9)	6.5	0.4	0.0	0.0	0.0	1.5275 (1.5237)	1.5324 (1.5289)	1.5337 (1.5303)	56.0	0.54	1
5	HEW-10	27.9 (28.7)	69.3 (71.3)	1.4	0.5	0.9	0.0	0.0	1.5258 (1.5242)	1.5313 (1.5298)	1.5328 (1.5314)	55.5	0.61	2, 3
6	SP-R(H)	39.6 (41.0)	56.9 (59.0)	3.4	0.1	0.0	0.0	0.0	1.5222 (1.5201)	1.5282 (1.5263)	1.5293 (1.5274)	49.8	0.62*	5, 6
7	SP-P(H)	43.4 (43.4)	56.5 (56.6)	0.1	0.0	0.0	0.0	0.0	1.5209 (1.5208)	1.5265 (1.5264)	1.5267 (1.5266)	15.0	0.50*	5, 6
8	439	43.8 (46.0)	51.4 (54.0)	3.8	0.0	0.1	0.0	0.9	1.5238 (1.5210)	1.5292 (1.5266)	1.5306 (1.5281)	53.3	0.59	5, 9
9	SP-N(H)	50.7 (51.1)	48.6 (48.9)	0.5	0.2	0.0	0.0	0.0	1.5202 (1.5198)	1.5255 (1.5251)	1.5258 (1.5254)	34.0	0.57*	5, 6
10	SP-M(H)	52.2 (53.2)	46.0 (46.8)	1.8	0.0	0.0	0.0	0.0	1.5206 (1.5195)	1.5255 (1.5245)	1.5263 (1.5253)	45.0	0.63*	5, 6
11	HEW-15	52.7 (55.4)	42.4 (44.6)	3.2	1.2	0.3	0.2	0.0	1.5223 (1.5193)	1.5269 (1.5242)	1.5274 (1.5247)	41.3	0.63	2, 3
12	HEW-4	57.6 (59.7)	38.9 (40.3)	2.0	1.1	0.3	0.1	0.0	1.5226 (1.5204)	1.5269 (1.5249)	1.5275 (1.5255)	41.8	0.60	2, 3
13	1909-261	59.7 (61.7)	37.1 (38.3)	1.7	1.1	0.3	0.0	0.1	1.5221 (1.5200)	1.5268 (1.5249)	1.5273 (1.5254)	35.3	0.59	5, 9
14	SP-J(H)	61.2 (61.8)	37.8 (38.2)	0.7	0.0	0.3	0.0	0.0	1.5191 (1.5185)	1.5240 (1.5234)	1.5240 (1.5235)	−16.0	0.52*	5, 6
15	SP-I(H)	64.0 (64.5)	35.2 (35.5)	0.8	0.0	0.0	0.0	0.0	1.5190 (1.5185)	1.5237 (1.5233)	1.5237 (1.5233)	0.0	0.55*	5, 6
16	SP-K(H)	66.2 (67.4)	32.0 (32.6)	1.6	0.0	0.2	0.0	0.0	1.5198 (1.5187)	1.5246 (1.5236)	1.5251 (1.5241)	20.0	0.58*	5, 6
17	HEW-13	66.7 (68.0)	31.3 (32.0)	1.7	0.0	0.0	0.3	0.0	1.5194 (1.5184)	1.5239 (1.5230)	1.5240 (1.5231)	21.8	0.61	2, 3
18	HEW-5	67.7 (71.6)	26.9 (28.4)	1.8	1.3	2.2	0.1	0.0	1.5235 (1.5203)	1.5277 (1.5247)	1.5283 (1.5253)	42.5	0.62	2, 3
19	HEW-3	69.8 (72.0)	27.1 (28.0)	0.1	2.8	0.2	0.0	0.0	1.5211 (1.5189)	1.5253 (1.5232)	1.5258 (1.5237)	35.8	0.65	2, 3
20	SP-G(H)	71.1 (73.1)	26.2 (26.9)	0.1	2.2	0.4	0.0	0.0	1.5199 (1.5180)	1.5247 (1.5229)	1.5242 (1.5224)	−29.0	0.53*	5, 6
21	SP-H(H)	71.1 (73.9)	25.1 (26.1)	1.9	1.7	0.2	0.0	0.0	1.5203 (1.5178)	1.5250 (1.5226)	1.5248 (1.5224)	−17.0	0.56*	5, 6
22	SP-F(H)	72.8 (74.3)	25.2 (25.7)	1.6	0.2	0.2	0.0	0.0	1.5192 (1.5180)	1.5240 (1.5229)	1.5236 (1.5225)	−28.0	0.54*	5, 6
23	HEW-2	74.0 (74.8)	24.9 (25.2)	0.8	0.1	0.1	0.1	0.0	1.5191 (1.5185)	1.5237 (1.5231)	1.5237 (1.5231)	0.0	0.60	2, 3
24	T-1	76.4 (77.4)	22.3 (22.6)	0.8	0.0	0.0	0.0	0.4	1.5201 (1.5193)	1.5252 (1.5245)	1.5248 (1.5241)	−17.0	0.59*	8
25	HEW-1	77.4 (79.8)	19.6 (20.2)	1.6	0.9	0.4	0.1	0.0	1.5206 (1.5187)	1.5248 (1.5230)	1.5248 (1.5230)	0.0	0.59	2, 3
26	HEW-12	79.2 (81.9)	17.5 (18.1)	2.2	0.6	0.2	0.3	0.0	1.5199 (1.5179)	1.5241 (1.5223)	1.5241 (1.5223)	−10.0	0.57	2, 3
27	SP-D(H)	80.9 (82.3)	17.4 (17.7)	1.2	0.3	0.2	0.0	0.0	1.5189 (1.5178)	1.5236 (1.5226)	1.5233 (1.5223)	−33.0	0.56*	5, 6
28	HEW-11	79.0 (83.8)	15.3 (16.2)	1.7	1.2	2.4	0.4	0.0	1.5228 (1.5195)	1.5269 (1.5239)	1.5270 (1.5240)	28.0	0.61	2, 3
29	7002H	83.1 (85.4)	14.2 (14.6)	0.5	1.3	0.0	0.0	0.9	1.5196 (1.5177)	1.5243 (1.5226)	1.5237 (1.5220)	−42.6	0.54	5, 9
30	SP-E(H)	85.6 (87.5)	12.2 (12.5)	0.9	1.1	0.2	0.0	0.0	1.5190 (1.5175)	1.5235 (1.5221)	1.5232 (1.5218)	−29.0	0.60*	5, 6
31	SP-C(H)	90.5 (91.5)	8.4 (8.5)	0.7	0.2	0.2	0.0	0.0	1.5187 (1.5180)	1.5233 (1.5227)	1.5227 (1.5220)	−44.8	0.56*	5, 6
32	SP-A(H)	92.6 (92.6)	7.4 (7.4)	0.0	0.0	0.0	0.0	0.0	1.5192 (1.5192)	1.5240 (1.5240)	1.5230 (1.5230)	−53.8	0.52*	5, 6

Note: For each sample, the adjusted composition, Or/(Or + Ab) and Ab/(Or + Ab), and the corrected refractive indices are given in parentheses beside their respective observed values. The negative signs of $2V_x$ values (in degrees) signify that the optic axial plane is parallel to (010). The Σt_1 values were derived either from lattice parameters b and c^* or from $2V_x$ and mole percent Or (marked *) using Fig. 2 in Su et al. (1986b). References are as follows: (1) DePieri and Quareni (1973); (2) Emerson and Guidotti (1974); (3) Hewlett (1959); (4) Smith (1958); (5) Smith and Ribbe (1966); (6) Spencer (1937); (7) Su et al. (1986a); (8) Tuttle (1952); (9) Warner et al. (1984).

Definitions

The symbols t_1o, t_1m, t_2o, t_2m are customarily used to designate the Al contents of the T_1O, T_1m, T_2O, T_2m tetrahedral sites of triclinic alkali feldspars (where t_i = the number of Al atoms in T_i sites divided by the total number of T_i sites). Thus, *high albite* (HA) is highly disordered and defined as $t_1o \gg t_1m \geq t_2o = t_2m$. There is no convention to exactly define "high" albite relative to "intermediate" albite. However, we have designated $\Sigma t_1 \equiv (t_1o + t_1m)$ as a measure of structural state and in this study used only specimens for which $0.5 \leq \Sigma t_1 \leq 0.65$. *Analbite* (AA) is also highly disordered and metrically triclinic, but it has $t_1o = t_1m$ and $t_2o = t_2m$ and thus can invert displacively to metrically monoclinic *monalbite* above the transition temperature (~980°C for pure, highly disordered $NaAlSi_3O_8$). The distinction between HA and AA is unimportant at this stage of our investigation.

For the K-rich series, monoclinic *high sanidine* (HS) has been defined traditionally on the basis of having its optic axial plane parallel to (010) [shorthand: O.A.P. = (010)]. Using data from crystals whose average composition was Or_{90}, Su et al. (1984) established the fact that $0.5 \leq \Sigma t_1 \leq 0.67$ for K-rich high sanidines. See Kroll et al. (1980) for further discussion of nomenclature.

Methods of determining structural state

To determine Σt_1 it is most desirable to have a neutron-diffraction refinement of the (Al,Si) distribution among nonequivalent tetrahedral sites or, failing that, an X-ray structure refinement. The latter involves interpretation of bond lengths in terms of Al content t_i of site T_i, and this is described at length in a review by Kroll and Ribbe (1983), who also prescribed methods of quantitatively estimating Σt_1 by using the demonstrated relationship among lattice parameters, mean T_i-O bond lengths, and Al contents of tetrahedral sites or pairs of sites, namely $\Sigma t_1 = (t_1o + t_1m)$ [note that $\Sigma t_2 = 1 - \Sigma t_1$]. The Kroll-Ribbe equations 10a and 10b have recently been revised using additional structural data plus a better algorithm for regression analysis. Accordingly, to estimate Σt_1 for specimens from lattice parameters, we use

$$\Sigma t_1 = 2t_1 = 72.245 - 3.1130b - 200.785c^*$$

for monoclinic feldspars and

$$\Sigma t_1 = t_1o + t_1m = \frac{b - 21.5398 + 53.8405c^*}{21.1567 - 15.8583c^*}$$

for triclinic feldspars (standard error of estimate is ±0.01

for assumed errors of ±0.002 Å in b and ±0.000 02 Å^{-1} in c^*; Kroll and Ribbe, in prep.).

In the absence of lattice parameters, we have used the optic axial angle $2V_X$ to estimate Σt_1, as discussed in detail by Su et al. (1986b). Fortunately, it is not extremely important for the present study that structural state be precisely known, because refractive indices are not extremely sensitive to variation in Σt_1, varying from as little as 0.000 01 to a maximum 0.000 06 per 0.01 Σt_1 in any isocompositional alkali feldspar series.

Labeling principal refractive indices

Probably the factor that has most obscured the true relationships between optical properties and composition in the HA(AA)–HS series is the same one that plagued the relationships between refractive indices and structural state for the K-rich alkali feldspar series, low microcline–high sanidine. The principal refractive index of a feldspar should be labeled, not α, β, and γ or n_α, n_β, and n_γ in the traditional manner, but n_a, n_b, and n_c according to which crystallographic axis **a, b,** or **c** the vibration direction is parallel or most nearly parallel. Hewlett's (1959) "b" corresponds to n_b, and in all alkali feldspars $n_a = n_\alpha$. For monoclinic high sanidines with O.A.P. = (010), $n_b = n_\beta$ and $n_c = n_\gamma$, but these are reversed for all other alkali feldspars, i.e., those with O.A.P. ⊥ (010) or approximately ⊥ (010) (Su et al., 1984; Bloss, 1985).

The data base

Choice of specimens

The 32 chemically analyzed alkali feldspars with $0.50 \leq \Sigma t_1 \leq 0.65$ selected for this study are listed in Table 1. They include a heated high albite from Ramona, California (J. R. Smith, 1958), two high albite single crystals prepared by heating a Clear Creek, California, specimen at high pressures (Su et al., 1986a), a highly disordered anorthoclase, whose structure was determined by DePieri and Quareni (1973), a homogeneous Eifel sanidine (Tuttle, 1952), the fourteen homogenized and "sanidinized" specimens of Spencer (1937) that had been heated for 100 to 300 h at 1075°C, and nine sanidines and one anorthoclase from Hewlett (1959). New data were added for a heated Eifel sanidine (7002H) and for two natural volcanic specimens (439 and 1909-261; Carmichael, 1965) by Warner et al. (1984), who determined optical properties and lattice parameters on the same single crystal. Because submicroscopic intergrowths have some small effects on refractive indices, we have attempted to use homogeneous feldspars for our investigation. To our knowledge we have allowed only two exceptions to this, namely Hewlett's specimens 4 and 15, which are described as having less than 5% exsolved Na-feldspar component (his Table 8, p. 527; see also powder-diffraction studies of the Hewlett specimens by Emerson and Guidotti, 1974).

Corrections for minor constituents

Chemical factors that obscure the relationship between refractive indices and Or content are the nonbinary constituents commonly found in minor amounts in high-temperature alkali feldspars. Hewlett (1959, p. 520f.) devised a simple linear method to correct his n_a indices (only) for the effects of iron content plus Ca-, Ba-, Sr-, and Rb-feldspar components. Our sources of mean refractive indices $\bar{n}_i$ were the same as his for $SrAl_2Si_2O_8$ (Srf), but differed for anorthite (An), celsian (Cn), $RbAlSi_3O_8$ (Rbf), and $KFeSi_3O_8$ (Fef); see Table 2. We used the following approach to calculate the corrected indices:

$$n^{corr}_{a,b,c} = n^{obs}_{a,b,c} - [(\bar{n}_i - \bar{n}^{obs}_{a,b,c})M_i/100],$$

where M_i is mole percent of the ith component and $\bar{n}^{obs}_{a,b,c}$ is the value of n_a, n_b, or n_c appropriate to the mole percent Or of a feldspar as determined from regression lines fitted to the observed indices (plotted in the upper portions of Figs. 1a, 1b, and 1c; lines not shown).

More refined values for $\bar{n}^{obs}_{a,b,c}$ could have been attained by iterative methods, and we tested two of the more "impure" specimens (Hew-11 and Hew-15) only to find that the final values of $n^{corr}_{a,b,c}$ changed insignificantly (by ±0.000 15 or less). Corrected indices are listed beside their respective observed values in Table 1. Corrected indices are plotted in the lower portions of Figures 1a, 1b, and 1c as a function of Or/(Or + Ab), whereas the observed values are plotted in the upper portions as a function of Or/(Or + Ab + An + Cn + Srf + Rbf).

Table 2. Refractive indices of some endmember feldspars

Endmember	n_α	n_β	n_γ	$\bar{n}$	Ref
$CaAl_2Si_2O_8$	1.5751	1.5838	1.5886	1.5825	2
$BaAl_2Si_2O_8$	1.589	1.593	1.599	1.594	4
$SrAl_2Si_2O_8$	1.574	1.582	1.586	1.581	3
$RbAlSi_3O_8$	1.520		1.529	1.525	1
$KFeSi_3O_8$	1.554	1.595	1.605	1.585	5

Note: The average structures of the alkaline-earth feldspars are disordered (Ribbe, 1984), the structural state of the Rb-feldspar is not known, and the Fe-feldspar is an "iron sanidine." References are as follows: (1) Boratskaya and Vlasova (1975) quoted by W. L. Brown (pers. comm.); (2) Burri et al. (1967); (3) Eskola (1922); (4) Roy (1965); (5) Wones and Appleman (1961).

Variation of refractive indices with composition

Warner et al. (1984) attempted to correlate n_a, n_b, and n_c with Or content for a few analyzed single crystals whose lattice parameters had been determined. In that preliminary study, effects of minor constituents were ignored, and linear regression lines showed that n_b and n_c crossed between Or_{70} and Or_{80}. However, it was observed that the n_c data were fit using a quadratic equation significantly better than with a linear one. Numerous unresolved questions led to this broader investigation using the 32 data sets described above. Indices, composition, and structural state were all measured on the same crystal for five of these, so it is obvious that some scatter in the relationships is to be expected. Moreover, scatter is inevitable because a rather wide range of structural states ($0.50 \leq \Sigma t_1 \leq 0.65$) was intentionally allowed, and some chemical zoning and

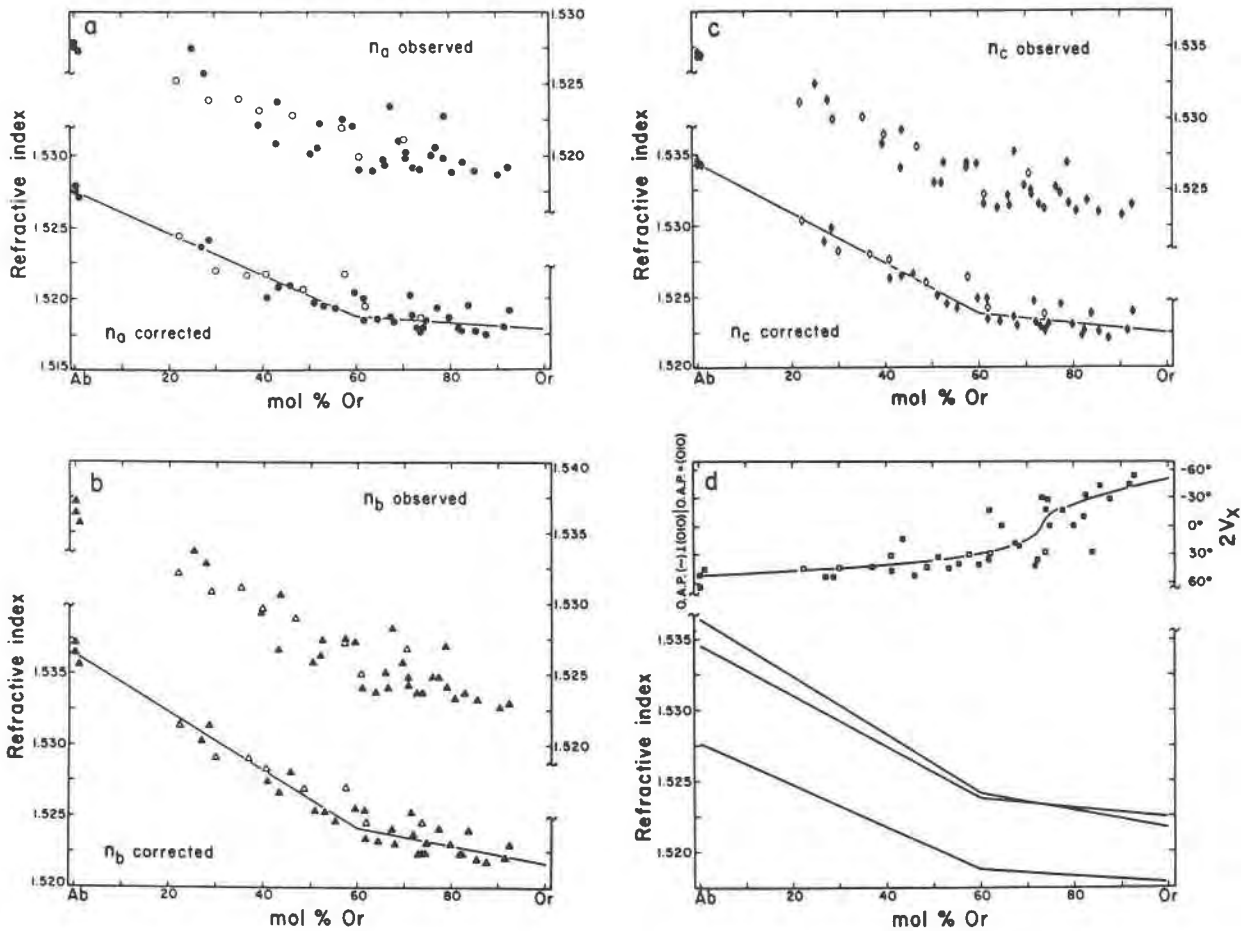

Fig. 1. Principal refractive indices as a function of composition for specimens with $0.5 \leq \Sigma t_1 \leq 0.65$: (a) n_a, (b) n_b, and (c) n_c. The upper portion of each figure displays the observed refractive indices plotted against Or/(Or + Ab + An + Cn + Srf + Rbf); the lower portions have indices corrected for minor constituents and are plotted against Or/(Or + Ab). Regression lines are drawn through the corrected data sets, segmented at Or_{60}. (d) The regression lines for HA–HS series from the three separate (a), (b), and (c) plots on the same scale, together with the observed $2V_x$ data points and the $2V_x$ curve calculated from the regression lines for refractive indices. Data in Tables 1 and 3. Solid symbols are for homogeneous specimens; open symbols are for unmixed specimens.

variation in structural state are expected from grain to grain within any bulk-analyzed sample (see especially Table 5 of Hewlett, 1959).

Plots of both the observed and the corrected n_a, n_b, and n_c indices versus Or content (Figs. 1a, 1b, and 1c) disclose negative slopes that are relatively steep from Or_0 to Or_{60} but much less steep from Or_{60} to Or_{100}. If a single curve were fitted to each full data set (Or_0 to Or_{93}), each would be concave upward and resemble Hewlett's plot of the index n_α versus Or content for (1) alkali feldspars from Or_{53} to Or_{93} that he had heated and homogenized to high structural states (see Hewlett's Fig. 2a) and (2) Spencer's

Table 3. Statistics for equations relating principal refractive indices to mole fraction of $KAlSi_3O_8$ ($\equiv X_{Or}$) for the samples in Table 1

Eq. no.	Or range (mol%)	Dep. var.	a_0	a_1	r^2	s	Predicted n		
							Or_0	Or_{60}	Or_{100}
1	0–60	n_a (n_α)	1.5276(5)	−0.0146(11)	0.951	0.0008	1.5276	1.5188	
2	0–60	n_c (n_β)	1.5345(3)	−0.0180(8)	0.984	0.0006	1.5345	1.5237	
3	0–60	n_b (n_γ)	1.5365(5)	−0.0205(11)	0.973	0.0008	1.5365	1.5242	
4	60–100	n_a (n_α)	1.5205(15)	−0.0026(19)	0.091	0.0008		1.5189	1.5179
5	60–100	n_c (n_β)	1.5257(14)	−0.0032(19)	0.137	0.0008		1.5238	1.5225
6	60–100	n_b (n_γ)	1.5280(17)	−0.0063(22)	0.319	0.0009		1.5242	1.5217

Note: The statistics were derived by linear least-squares regression methods ($n_i = a_0 + a_1 X_{Or}$). The numbers in parentheses are standard errors referring to last digit(s). Coefficient of determination r^2, square root of mean errors s, and predicted values for Or_0, Or_{60} and Or_{100} are also listed. The very small r^2 values for the range Or_0–Or_{60} are due to the very limited range of the independent variable X_{Or}.

(1937) data (see Hewlett's Fig. 2b) that cover a slightly broader range (Or_{40} to Or_{92}).

The preceding trends relating refractive indices to Or content find corroboration in terms of the variation of density with Or content. Densities of the high albite (analbite)–high sanidine series have been studied by Spencer (1937), Barth (1969), and Smith (1974, Fig. 12-15). Using unit-cell volumes and compositions for well-characterized LA–LM (low albite–low microcline) and AA–HS exchange series from Kroll et al. (1986, Tables 4 and 5), theoretical densities were calculated and plotted in Figure 2 versus mole percent Or for both the low- (LA–LM) and high-temperature (AA–HS) series. The trends in Figure 2, which resemble those in Smith's Figure 12-15, mimic those in Figures 1a, 1b, and 1c. This is not surprising because it is well known that, in general, refractive index and density vary sympathetically.

Although polynomial curves best fit the density versus composition data, we arbitrarily chose Or_{60} as a flexure point in Figure 2 and assumed that Or_{60} also marked a flexure point in the index versus composition data (Figs. 1a, 1b, and 1c). Accordingly, least-squares regressions were performed on the refractive-index data between Or_0 and Or_{60} and between Or_{60} and Or_{100}. The six lines shown in Figures 1a, 1b, and 1c, whose intercepts (a_0) and slopes (a_1) are listed in Table 3, were thus obtained. Whether these six linear relationships truly prevail remains moot. On the other hand, if n_a, n_b, or n_c is predicted for the composition Or_{60} using the line from Or_0 to Or_{60} line and, again, using the line from Or_{60} to Or_{100}, the values agree to within ± 0.0001 (Table 3).

The mean refractive index ($\bar{n}$) of our corrected n_a, n_b, and n_c refractive indices equals 1.5329 for high albite (Or_0) and 1.5207 for high sanidine (Or_{100}), whereas their densities (ρ), as calculated from the data of Kroll et al. (1986), are 2.615 g/cm³ (Or_0) and 2.555 g/cm³ (Or_{100}). Inserting these values into the left side of the Gladstone-Dale relationship

$$\frac{\bar{n} - 1}{\rho} = \Sigma k_i \xi_i,$$

where k_i is the Gladstone-Dale "constant" and ξ_i is the weight fraction of the ith oxide (see Larsen, 1921), the quotient $(\bar{n} - 1)/\rho$ equals 0.2038 in both cases. The precise equality trends to corroborate the corrected values for n_a, n_b, and n_c, as well as the calculated densities.

Note that in Figure 1d the n_b and n_c curves cross at about Or_{73}, where $2V_X = 0°$ and the optic axial plane changes from O.A.P. approximately $\perp$ (010) to O.A.P. = (010). This intersection will vary, depending on the average structural state of the data set (Su et al., 1986b, Fig. 2). In this case Or_{73} is the value for specimens that have an average Σt_1 of 0.60.

Conclusions

Although our fitting of two linear segments to the refractive indices of these high alkali feldspars is an approximation, it is probably all that the data can substantiate. More sophisticated treatment would require a series of data sets for which indices, $2V$, structural state, and bulk composition had each been measured on the same crystal. The work involved in such an undertaking would seem unjustified in the light of the present results. Even if better curves for n_a, n_b, and n_c versus mole percent Or were to be produced, they would have no practical application.

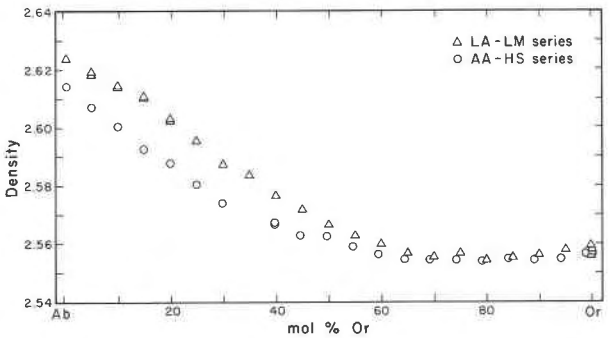

Fig. 2. Variations of density with mole percent Or for the LA–LM and the AA–HS alkali-exchange series. Densities were calculated from unit-cell volumes and compositions reported by Kroll et al. (1986, Tables 4 and 5).

The curve plotted in Figure 1d represents the variation of optic axial angle $2V_X$ with Or/(Or + Ab) as calculated from the equations of n_a, n_b, and n_c, summarized in Table 3. If the observed $2V_X$ values for the 32 specimens (Table 1) are plotted in Figure 1d, the scatter is great and is due almost exclusively to differences in the structural states of the specimens used for determining the refractive-index curves. This is discussed in detail by Su et al. (1986b).

Acknowledgments

This work was supported in part by National Science Foundation Grant EAR-83-08308 to F.D.B. and P.H.R. S.C.S. gratefully acknowledges financial support from N.S.F. and a Cunningham Fellowship awarded by Virginia Polytechnic Institute and State University. We are grateful to H. Wondratschek of Universität Karlsruhe, West Germany, and especially to D. B. Stewart of the U.S. Geological Survey, Reston, Virginia, for comments and constructive criticism. We appreciate the helpful reviews of this manuscript by G. L. Hovis and P. Černý.

References

Bambauer, H.U., Taborszky, F., and Trochim, H.D. (1979) Optical determination of rock-forming minerals. Part 1. Determinative tables. Schweizerbart'sche Verlagsbuchhandlung, Stuttgart, 188 p.

Barth, T.F.W. (1969) Feldspars, 261 p. Wiley, New York.

Bloss, F.D. (1985) Labelling refractive index curves for mineral series. American Mineralogist, 70, 428–432.

Burri, C., Parker, R.L., and Wenk, E. (1967) Die optische Orientierung der Plagioklase—Unterlagen und Diagramme zur Plagioklasbestimmung nach der Drehtische-methode, 334 p. Birkhauser, Basel and Stuttgart.

Carmichael, I.S.E. (1965) Trachytes and their feldspar phenocrysts. Mineralogical Magazine, 34, 107–125.

Deer, W.A., Howie, R.A., and Zussman, J. (1963) Rock-forming

minerals. 4. Framework silicates, 435 p. Longmans, Green and Co., London.
DePieri, R., and Quareni, S. (1973) The crystal structure of an anorthoclase: An intermediate alkali feldspar. Acta Crystallographica, B29, 1483–1487.
Eskola, P. (1922) The silicates of strontium and barium. American Journal of Science, series 5, 4, 331–375.
Emerson, R.W., and Guidotti, C.F. (1974) New X-ray and chemical data on Hewlett's 1959 feldspar suite. American Mineralogist, 59, 615–617.
Hewlett, C.G. (1959) Optical properties of potassic feldspars. Geological Society of America Bulletin, 70, 511–538.
Kroll, H., and Ribbe, P.H. (1983) Lattice parameters, composition and Al,Si order in alkali feldspars. Mineralogical Society of America Reviews in Mineralogy, 2, 2nd edition, 57–100.
Kroll, H., Bambauer, H.-U., and Schirmer, U. (1980) The high albite–monalbite and analbite-monalbite transitions. American Mineralogist, 65, 1192–1211.
Kroll, H., Schmiemann, I., and Cölln, G. von. (1986) Feldspar solid solutions. American Mineralogist, 71, 1–16.
Larsen, E.S. (1921) The microscopic determination of the nonopaque minerals. U.S. Geological Survey Bulletin 679, 294 p.
Phillips, W.R., and Griffen, D.T. (1981) Optical mineralogy. The nonopaque minerals, 677 p. Freeman, San Francisco.
Ribbe, P.H. (1984) Average structures of plagioclase and alkali feldspars: Systematics and applications. In W.L. Brown, Ed. Feldspars and feldspathoids: Structures, properties and occurrences, 541 p. NATO Advanced Study Institute, Series C, 137, D. Riedel, Dordrecht.
Roy, N.N. (1965) The mineralogy of the potassium-barium feldspars series. I. The determination of the optical properties of natural members. Mineralogical Magazine, 35, 508–518.
Shelley, D. (1985) Manual of optical mineralogy. Second edition, 321 p. Elsevier, New York.
Smith, J.R. (1958) Optical properties of heated plagioclases. American Mineralogist, 43, 1179–1194.
Smith, J.V. (1974) Feldspar minerals. I. Crystal structure and physical properties, 627 p. Springer-Verlag, Heidelberg.
Smith, J.V., and Ribbe, P.H. (1966) X-ray-emission microanalysis of rock-forming minerals. III. Alkali feldspars. Journal of Geology, 74, 197–216.
Spencer, E. (1937) The potash-feldspars I. Thermal stability. Mineralogical Magazine, 24, 453–494.
Su, S.C., Bloss, F.D., Ribbe, P.H., and Stewart, D.B. (1984) Optic axial angle, a precise measure of Al,Si ordering in T_1 tetrahedral sites of K-rich alkali feldspars. American Mineralogist, 69, 440–448.
Su, S.C., Ribbe, P.H., Bloss, F.D., and Goldsmith, J.R. (1986a) Optical properties of single crystals in the order-disorder series low albite–high albite. American Mineralogist, 71, 1384–1392.
Su, S.C., Ribbe, P.H., and Bloss, F.D. (1986b) Alkali feldspars: Structural state determined from composition and optic axial angle $2V$. American Mineralogist, 71, 1285–1296.
Tuttle, O.F. (1952) Optical studies on alkali feldspars. American Journal of Science, Bowen volume, 553–568.
Warner, J.K., Su, S.C., Ribbe, P.H., and Bloss, F.D. (1984) Optical properties of the analbite–high sanidine solid solution series. Geological Society of America Abstracts with Programs, 16, 687.
Wones, D.R., and Appleman, D.E. (1961) X-ray crystallography and optical properties of synthetic monoclinic $KFeSi_3O_8$, iron-sanidine. U.S. Geological Survey Professional Paper 424-C, 309–310.

Manuscript received April 23, 1986
Manuscript accepted August 6, 1986